

# UNDERSTANDING ANODE OVERPOTENTIAL

Rebecca Jayne Thorne<sup>1</sup>, Camilla Sommerseth<sup>1</sup>, Ann Mari Svensson<sup>1</sup>, Espen Sandnes<sup>2</sup>, Lorentz Petter Lossius<sup>2</sup>, Hogne Linga<sup>2</sup>, and Arne Petter Ratvik<sup>1</sup>

<sup>1</sup>Dept. of Materials Science and Engineering, Norwegian University of Science and Technology, NO-7491 Trondheim, Norway  
<sup>2</sup>Hydro Aluminium, Årdal, Norway

Keywords: Anode, carbon, electrochemistry, characterisation, overpotential.

## Abstract

In aluminium electrolysis cells the anodic process is associated with a substantial overpotential. Industrial carbon anodes are produced from a blend of coke materials, but the effect of coke type on anodic overpotential has not been well studied. In this work, lab-scale anodes were fabricated from single cokes and electrochemical methods were subsequently used to determine the overpotential trend of the anode materials. Attempts were then made to explain these trends in terms of both the physical and chemical characteristics of the baked anodes themselves and their raw materials. Routine coke and anode characterisation methods were used to measure properties such as impurity concentrations and reactivity (to air and CO<sub>2</sub>), while non-routine characterisation methods were applied to study other surface and structural properties. It was found that the overpotential trend of the anodes correlated well with many of the properties studied, and explanations for these observed correlations are suggested. These findings offer exciting possibilities for reducing the energy demand of the anodic process.

## Introduction

The overall potential of a typical industrial aluminium cell is around 4.6 V [1]. The total voltage associated with the anode is around 1.5-1.8, referred to the aluminium potential, of which 0.3-0.6 V is derived from overpotential [1]. Anodic overpotential is composed of three parts – reaction overpotential, concentration overpotential and bubble overpotential (or resistance). Concentration overpotential is thought to be very low at normal current densities, so the overpotential under normal operational conditions mainly comprises of reaction and bubble overpotential [1]. Reducing these components is consequently desirable to decrease the energy demand and production cost of aluminium.

Although the magnitude of anode overpotential has been studied in various melt and set-up conditions, few detailed studies of the relationship of overpotential to anode material properties (chemical and physical) have been performed. Electrocatalysts such as iron, vanadium and calcium have been found both to increase air and CO<sub>2</sub> reactivity [2-5] and cause increased electrolytic anode consumption and/or decreased overpotential [1, 4, 6-8]. However, electrocatalyst studies have mostly focused on artificially doped anode materials which do not necessarily reflect the real situation found in cokes. Additionally, various papers have investigated how changes in physical coke properties, such as structure and density, have affected anode performance, but

have not linked these coke properties to overpotential directly [2, 9-11]. It is likely that coke and anode physical properties will have an effect on overpotential, as the reactivity of carbons, both electrochemical reactions and oxidation reactions, is generally known to be related to microstructural parameters [12, 13]. In addition, the formation and release of CO<sub>2</sub> bubbles also relies on the surface microstructure [14].

In a previous study that served as preliminary work on a new project, the total overpotential of a range of carbon anodes varying only in coke type was measured [15]. These anodes were labeled 1 to 4, and a distinct overpotential trend was found with anode 4 having a lower overpotential than anode 1 by approximately 200 mV at 1 A cm<sup>-2</sup>. Overpotential was found to correlate well with the concentration of metal impurities (electrocatalysts) and total sulphur in the anode, but relationships with other anode properties were not studied. As unshielded rods were used as the anode design (which were immersed in the melt approximately 1.5 cm), other limitations of the initial study included the fact that the immersed anode area was undefined, the current distribution was not equal over the active anode surface and bubbles trapped underneath the anode create noise in the electrochemical measurements and extra bubble resistance. This paper follows up and expands on the previous study, studying the overpotential of the same series of anode materials. The method with which to study overpotential was improved and further efforts were made to understand the differences in overpotential observed. Correlations of overpotential with some of the main industrial methods traditionally used to characterise anodes (air and CO<sub>2</sub> reactivity) were also investigated.

## Materials and Methods

Four types of single cokes were used to produce pilot scale anodes with a fraction size of 0-2 mm; these were labeled anodes 1 to 4. The production of the anodes varied only in the coke type, all other parameters were kept constant. A graphite material was also used for a comparison with the industrial style anodes. For electrochemical testing, anodes were cut and assembled as schematically depicted in Figure 1. Immersed anode area was defined using boron nitride (BN) shielding. Thus, advantages over the previous anode design (from [15]) included a defined surface area to be immersed in the melt (1.5 cm<sup>2</sup>), an even current distribution and a minimised bubble retention due to the vertical surface. The impact of anode geometry was directly compared by also including an unshielded graphite rod in the measurement series, as used in [15]. This is shown in figure 2.

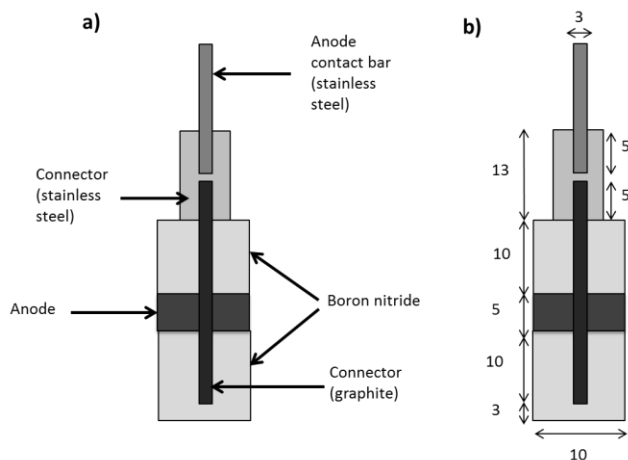


Figure 1. The anode assembly used in this study. All materials were threaded together on a 3 mm graphite rod, which was attached via a connector piece to a stainless steel contact bar. The BN shields defined an active anode surface area of  $1.6 \text{ cm}^2$ . b. with dimensions (mm)

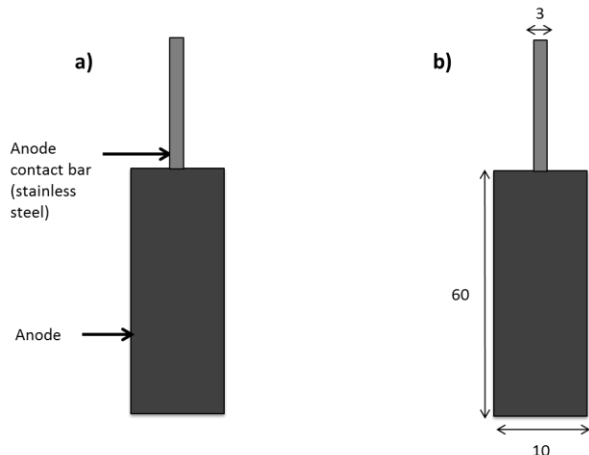


Figure 2. The anode assembly used in [15], which was also used in this study to investigate the impact of anode geometry on electrochemical measurements. When immersed 1.5 cm in the melt, this had an approximate active anode surface area of  $5.5 \text{ cm}^2$ . b. with dimensions (mm)

Experiments were performed in a cryolite melt (cryolite ratio = 2.3 (cryolite from Sigma Aldrich, purity >97 %), with excess  $\text{AlF}_3$  equal to 9.8 wt% (industrial grade  $\text{AlF}_3$  sublimed in-house) and an alumina concentration of 9.4 wt%, ( $\gamma$  alumina from Merck). The melt was contained in a graphite crucible (Svensk Specialgrafit AB, Sweden) in which an alumina disk was placed. An aluminium reference electrode in an alumina assembly was fabricated according to [16]. A schematic of the overall experimental setup is shown in Figure 3.

All electrochemistry was performed using a Zahner IM6 (with built in EIS module and 10 A booster PP201, all from Zahner-Elektrik). Electrochemical Impedance Spectroscopy (EIS) was used to determine the ohmic resistance at the Open Circuit Potential (OCP), the value of which was used to  $iR$  compensate all

electrochemical measurements. A current density (CD) of  $1 \text{ A cm}^{-2}$  was then applied to each anode and the potential measured (relative to an aluminium reference electrode) for 200 seconds, before repeating. This CD of  $1 \text{ A cm}^{-2}$  was chosen as it is close to the anode CD in modern industrial cells. Polarisation curves were also recorded for each anode by slowly sweeping the anode potential from the OCP to 2.5 V at  $0.1 \text{ V s}^{-1}$  and measuring the responding current.

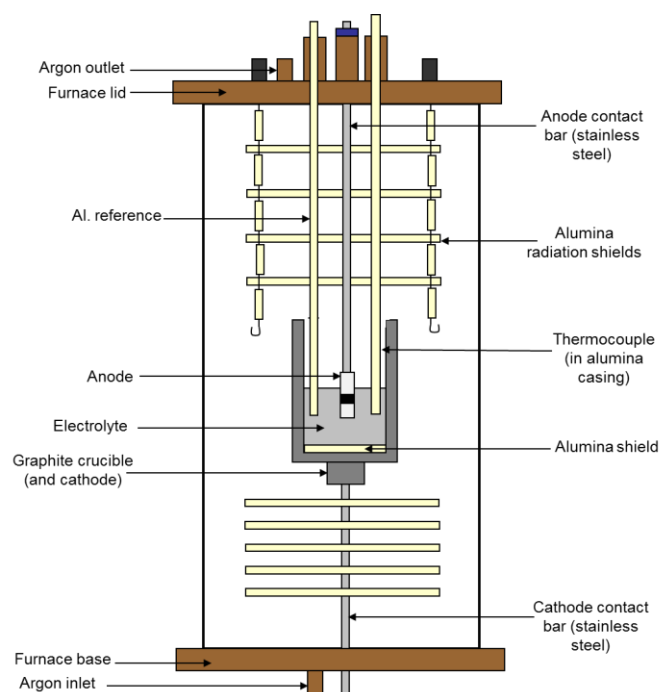


Figure 3. The furnace and crucible setup.

The order of the anode materials tested was randomised to eliminate possible changing characteristics of the melt over time, and two parallels were performed for each material (with new anodes) in the same bath. Bath samples after each anode experiment were taken for subsequent oxide content analysis (LECO analyser model TC-436DR).

Anode materials were additionally characterised according to routine industrial methods (including air and  $\text{CO}_2$  reactivity), and additionally for structure. Isotropy of the anodes was studied using optical microscopy (under polarised light) after mounting anodes in epoxy and polishing to  $1 \mu\text{m}$ . To further study the relative amount of surface active sites, the oxygen content of the samples was measured using LECO analysis between room temperature and  $2800^\circ\text{C}$ . For the LECO analysis, fines were produced with a size of  $<63 \mu\text{m}$ .

## Results and Discussion

### Overpotential measurements

Comparison of the potential at  $1 \text{ A cm}^{-2}$  in Table 1 showed a variation of 0-120 mV for repeats of the same material, whilst the potential between different materials was found to vary by an average of 140-310 mV. The variation in potential between

repeats was possibly due to the inhomogeneous nature of the anode material as only small samples were used. However, as the repeat variation was lower than the differences between materials, the overpotential trends were confirmed and were not experimental error. The order of the materials was also identical to that found in the previous paper [15]; Anode 4 had the lowest potential at  $1 \text{ A cm}^{-2}$  (and therefore the lowest overpotential), compared to graphite which had the highest potential. Polarisation curves additionally supported this trend, showing the same magnitude differences between anode materials at  $1 \text{ A cm}^{-2}$ . The polarisation curves also showed that this trend was the same at both lower and higher current densities, and the onset potential for  $\text{CO}_2$  production was  $\sim 300 \text{ mV}$  lower in Anode 4 than in graphite (Figure 4). LECO measurements of all the melt samples showed little variation in alumina concentration over the course of the experiments, meaning all potential differences could be considered due to the materials only. Owing to the fact that all anodes had identical distribution of grain size and pitch type/level, these variations in potential must relate to differences in the coke properties.

Table 1. Potentials of the anodes after 200 seconds at  $1 \text{ A cm}^{-2}$ .

Material	Potential at $1 \text{ A cm}^{-2} / \text{V}$			Overpotential (high to low)
	Repeat 1	Repeat 2	Average and ST DEV	
Graphite	1.57	1.57	1.57 +/- 0.00	↓
Anode 1	1.45	1.40	1.43 +/- 0.04	
Anode 2	1.39	1.38	1.38 +/- 0.01	
Anode 3	1.30	1.37	1.34 +/- 0.05	
Anode 4	1.20	1.32	1.26 +/- 0.08	

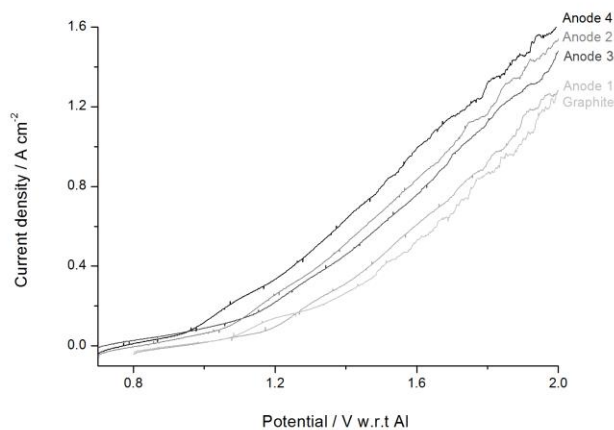


Figure 4. Polarisation curves of graphite and anodes 1 to 4 recorded at  $0.1 \text{ V s}^{-1}$ . From left to right: Anode 4 (black), Anode 2 (medium grey), Anode 3 (dark grey), Anode 1 (grey) and graphite (light grey). Only forward scans from OCP to  $2 \text{ V}$  are shown for clarity.

The effect of anode geometry was studied by comparing the new anode design with the defined vertical surface with an unshielded rod with both vertical and horizontal surfaces, as used in [15] (Figures 1 and 2). Graphite was the anode material for both designs. When the potential measured over time at  $1 \text{ A cm}^{-2}$  was

compared (Figure 5), there was much less oscillation noise of the potential with the new vertical anode design. It is likely that the noise difference is due to bubbles trapped on the horizontal surface of the unshielded rod [14]; as the bubbles grow in size they cover more of the anode surface causing the potential to increase as local CD increases. When the bubble escapes the local CD is normalised and the potential abruptly decreases. The new anode design is therefore superior for measuring overpotential trends.

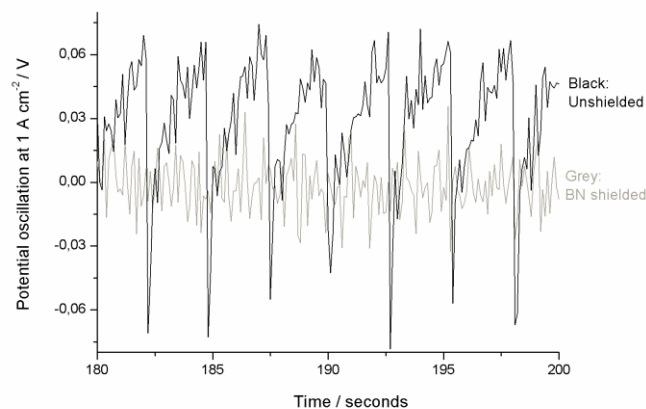


Figure 5. Potential in volts measured at a graphite anode at  $1 \text{ A cm}^{-2}$ , normalised around zero to show oscillation. Measurements were performed with either the new BN shielding with only a vertical surface (grey), or an unshielded rod with both vertical and horizontal surfaces (black).

### Correlations with the overpotential trend

As described in the previous paper, [15], the decreasing overpotential trend correlates well with increasing levels of metals and sulphur. For example, anode 4 had the lowest overpotential and the highest total concentrations of metals and sulphur. As metallic impurities can catalyse air and  $\text{CO}_2$  reactivity, it makes sense that these can additionally catalyse the anode reaction and reduce overpotential [1]. However, the chemical properties of an anode are just one possible contributor to the variation in overpotential.

Microstructure was studied by observing polished cut-sections of the anodes under polarised light with optical microscopy, as shown in Figure 6. A clear trend of increasing isotropy was observed from graphite and Anode 1, to Anode 4, as evidenced by a decrease in crystallinity and an increase in fineness. The increase in boundaries or 'edges' between crystallites makes it possible that Anodes 3 and 4 have a higher level of electrochemically active sites than anodes 1, 2 and graphite. This offers another possible explanation of the overpotential differences between the materials.

Another way of characterising the active site content is through the oxygen content of the anodes; as active sites are known to become oxidised [13], measuring the amount of oxygen in a graphitic sample can indicate the relative amount of active sites on

the surface. LECO combustion analysis results indicated that increasing levels of oxygen were found from Anodes 1 to 4 (Figure 7). Comparable levels of oxygen were found in each anode and in the corresponding coke used to make it, although anodes had slightly higher oxygen levels than their coke. A reason for this is not clear, but could be due to the added pitch or additional changes to the carbon during anode baking. The oxygen trend found supports the idea that Anodes 3 and 4 could have higher levels of active sites on their surface, but as these anodes also have the highest levels of metallic impurities [15], the contribution from metal oxides to the total oxygen content measured by LECO cannot be ruled out.

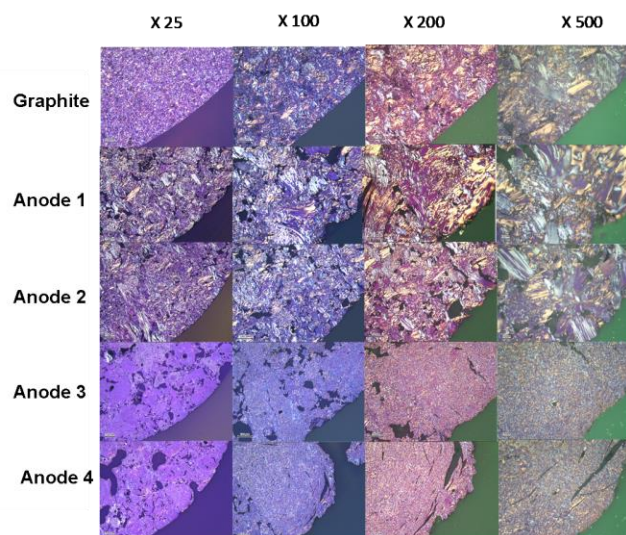


Figure 6. Optical microscopy images (under polarised light) of anodes mounted in epoxy and polished down to 1  $\mu\text{m}$ .

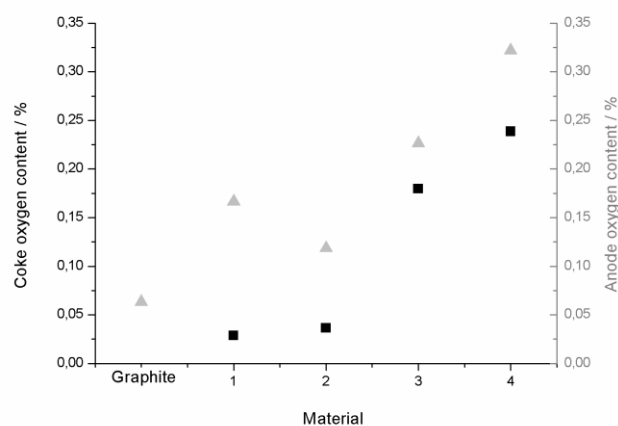


Figure 7. Total oxygen content of the cokes (black squares) and their corresponding anodes (grey triangles). Graphite is also shown for a comparison.

The quality of an anode is routinely measured and compared in industry using properties such as air and  $\text{CO}_2$  reactivity. The lower the air and  $\text{CO}_2$  reactivity, the less consumption and the better performance an anode is considered to have [16]. Analysis results for air and  $\text{CO}_2$  reactivity are shown in Table 2. It was

shown that Anodes 3 and 4 have the highest air reactivity and low  $\text{CO}_2$  reactivity. The fact that Anodes 3 and 4 have the lowest overpotential and the highest air reactivity is interesting; this correlation could make sense if it is assumed that the nature of the electrochemical oxidation of the anode with an oxygen species (i.e. derived from alumina, in the electrochemical reaction), and the thermal oxidation of carbon with oxygen in air is of the same nature.

Table 2. Anode air and  $\text{CO}_2$  reactivity.

Material	Reactivity / $\text{mg cm}^{-2} \text{h}^{-1}$	
	R(air)	R( $\text{CO}_2$ )
Graphite	-	-
Anode 1	39.0	19.0
Anode 2	29.5	5.9
Anode 3	69.5	7.2
Anode 4	70.1	7.4

The main findings of this paper, including the overpotential trend of the anodes and the correlation of overpotential with other properties studied, are summarised in table 3

Table 3. The relationship of overpotential to impurities, isotropy, oxygen content and air reactivity.

Material	$\eta$	Total impurities	Isotropy	O content	R(air)
Graphite	↓	↓	↓	↓	↓
Anode 1	↓	↓	↓	↓	↓
Anode 2	↓	↓	↓	↓	↓
Anode 3	↓	↓	↓	↓	↓
Anode 4	↓	↓	↓	↓	↓

## Conclusions

Overpotential was found to vary by as much as 170 mV between four anodes varying only in coke type, confirming the trends found in [15]. When graphite was also included in the comparison, the variation in potential was 310 mV. The anodes in this study had no horizontal surfaces; this design was shown to lower the voltage oscillation when compared to unshielded rods with both vertical and horizontal surfaces, most likely due to a reduction in bubble coverage.

Relationships were found between the overpotential trend of the anodes and anode impurity level, isotropy and oxygen content, as summarised in Table 3. Electrocatalyst impurities have been linked to a decrease in overpotential in previous publications. Increasing isotropy levels and an increase in oxygen could indicate an increase in active sites on the anode surface. Although this is as yet unproven, variations in relative concentrations of electrochemically-active sites could also explain the trend in overpotential observed. Overpotential was additionally compared with anode air and  $\text{CO}_2$  reactivity; two properties which are routinely used in industry as indicators of anode performance. Overpotential correlated reasonably well with air reactivity. If this relationship is real, it could be that optimising an anode for its

electrochemical properties (overpotential) is a trade-off for higher air reactivity.

At present, it is unknown whether metal impurities or variations in active sites have a dominant effect on overpotential. Additionally, due to the fact that other properties vary between anode types, further important factors towards overpotential could include porosity, surface morphology, real surface area or electrolyte wetting properties, not discussed in this paper.

### Acknowledgements

This work was financed by Hydro Aluminium and the Research Council of Norway. Thanks are due to Aksel Alstad at the NTNU workshop where fabrication of experimental parts was required, as well as to Hydro Aluminium lab engineers at Årdalstangen for performing XRF and reactivity (to air and CO<sub>2</sub>) testing. Additionally, the contributions of Egil Skybakmoen and others at SINTEF are gratefully acknowledged.

### References

1. Thonstad, J., Fellner, P., Haarberg, G.M., Hives, J., Kvande, H., and Sterten, Å., *Aluminium Electrolysis* 3rd edition ed. 2001, Breuerdruck, Germany: Aluminium-Verlag Marketing & Kommunikation GmbH.
2. Leach, C.T., Brooks, D.G., and Gehlbach, R.E., *Correlation of Coke Properties, Anode Properties and Carbon Consumption*. Light Metals, 1997.
3. Rolle, J.G. and Hoang, Y.K., *Studies of Vanadium and Sodium on the Air Reactivity of Coke and Anodes*. Light Metals, 1995.
4. Kuang, H., Thonstad, J., and Sørli, M., *Effects of Additives on the Electrolytic Consumption of Carbon Anodes in Aluminium Electrolysis*. Carbon, 1995. **33**(10).
5. Sørli, M. and Eidet, T., *The Influence of Pitch Impurity Content on Reactivity of Binder Coke in Anodes*, in *Light Metals*. 1998. p. 763-768.
6. Feng, N., Zhang, M., Grjotheim, K., and Kvande, H., Carbon, 1991. **29** (1): p. 39-42.
7. Liu, Y., Wang, X., Huang, Y., Yang, J.H., and Wang, W., in *Light Metals*. 1995. p. 247-251.
8. Haarberg, G.M., Solli, L.N., and Sterten, Å. in *7th Slovak Aluminium Symp.* 1993. Bankska Bystrica.
9. McClung, M. and Ross, J.A., *A Method to Correlate Raw Material Properties to Baked Anode Core Performance*. Light Metals, 2000.
10. Wilkening, S., *Maintaining Consistent Anode Density Using Varying Carbon Raw Materials*. Light Metals, 2009.
11. Samanos, B. and Dreyer, C., *Impact of Coke Calcination Level and Anode Baking Temperature on Anode Properties*. Essential Readings in Light Metals: Electrode Technology for Aluminum Production. **4**.
12. Banks, C.E., Davies, T.J., Wildgoose, G.G., and Compton, R.G., *Electrocatalysis at graphite and carbon nanotube modified electrodes: edge-plane sites and tube ends are the reactive sites*. Chem. Commun., 2005.
13. Laine, N.R., Vastola, F.J., and Walker, P.L.J., *The Importance of Active Surface Area in the Carbon-Oxygen Reaction*. Journal of Physical Chemistry, 1963. **67**.
14. Einarsrud, K.E. and Johansen, S.T., *Modelling of bubble behavior in aluminium reduction cells*. Progress in Computational Fluid Dynamics, 2012. **12**(2): p. 119-130.
15. Thorne, R.J., Sommerseth, C., Sandnes, E., Kjos, O.S., Aarhaug, T.A., Lossius, L.P., Linga, H., and Ratvik, A.P., *Electrochemical characterization of carbon anode performance*. Light Metals, 2013.
16. Lhuissier, J., Bezamanifary, L., Gendre, M., and Chollier, M.-J., *Use of under calcined coke for the production of low reactivity anodes*. Light Metals, 2009.